

UNCLASSIFIED

AD NUMBER

AD816215

LIMITATION CHANGES

TO:

Approved for public release; distribution is unlimited.

FROM:

Distribution authorized to U.S. Gov't. agencies and their contractors;
Administrative/Operational Use; 28 JUN 1967.
Other requests shall be referred to Air Force Technical Applications Center, Washington, DC.

AUTHORITY

DARPA ltr 1 May 1972

THIS PAGE IS UNCLASSIFIED

AD816215

**MULTIPLE COHERENCE OF NOISE
AT 3 VERTICAL ARRAYS
UBSO, GV-TX, AP-OK**

28 June 1967

Prepared For

**AIR FORCE TECHNICAL APPLICATIONS CENTER
Washington, D. C.**

By

**E. F. Chiburis
W. C. Dean**

TELEDYNE, INC.

Under

Project VELA UNIFORM

Sponsored By

**ADVANCED RESEARCH PROJECTS AGENCY
Nuclear Test Detection Office
ARPA Order No. 624**

MULTIPLE COHERENCE OF NOISE

AT 3 VERTICAL ARRAYS

UBSO, GV-TX, AP-OK

SEISMIC DATA LABORATORY REPORT NO. 191

AFTAC Project No.:	VELA T/6702
Project Title:	Seismic Data Laboratory
ARPA Order No.:	624
ARPA Program Code No.	5810

Name of Contractor:	TELEDYNE, INC.
---------------------	----------------

Contract No.:	F 33657-67-C-1313
Date of Contract	2 March 1967
Amount of Contract:	\$ 1,736,617
Contract Expiration Date:	1 March 1968
Project Manager:	William C. Dean (703) 836-7644

P. O. Box 334, Alexandria, Virginia

AVAILABILITY

This document is subject to special export controls and each transmittal to foreign governments or foreign national may be made only with prior approval of Chief, AFTAC.

This research was supported by the Advanced Research Projects Agency, Nuclear Test Detection Office, under Project VELA-UNIFORM and accomplished under the technical direction of the Air Force Technical Applications Center under Contract F 33657-67-C-1313.

Neither the Advanced Research Projects Agency nor the Air Force Technical Applications Center will be responsible for information contained herein which may have been supplied by other organizations or contractors, and this document is subject to later revision as may be necessary.

TABLE OF CONTENTS

	Page No.
ABSTRACT	
1. INTRODUCTION	1
2. DESCRIPTION OF DATA	4
3. RESULTS	5
Multiple Coherence	5
Stationarity Tests	8
4. CONCLUSIONS	10
FIGURES	
APPENDIX 1	1-1
Multiple Coherence Functions	
APPENDIX 2	2-1
Theoretical Development of The Stationarity Relations	
A. Noise Reduction Within The Fitting Interval	2-1
B. Noise Reduction Outside The Fitting Interval	2-3
REFERENCES	

ABSTRACT

Multiple coherence gives a quantitative measure versus frequency of how well a linear combination of n input channels can match the $(n + 1)$ st channel in a seismic array. If the inputs can match the output exactly, then the multiple coherence is unity and only n channels are necessary to describe the noise field. This report shows multiple coherence versus frequency at three vertical arrays of short period, vertical component seismometers. One of the seismic traces, either the surface trace or the deepest trace, is used as the output and 2 to 6 of the others are used as inputs.

The multiple coherence properties of the noise are similar at the three vertical arrays with similar geometries. At all three sites the downhole channels correlate with each other better than with the surface channel. At all three sites the coherence between downhole seismometers decreases markedly as their separation increases.

When the deep trace is the output and all seismometers are added as inputs, the multiple coherence is highest at GV-TX. The multiple coherence at GV-TX is greater than .85 for all frequencies from .1 to 2.5 cps. For the AP-OK and UBSO wells the multiple coherence varies between .6 to .9 for most frequencies greater than .5 cps.

1. INTRODUCTION

Most basic data processing techniques for signal enhancement or identification depend upon the structure of the noise within the seismic array. If some of the coherent noise is due to site characteristics such as consistently coherent noises from particular directions, then techniques using multiple coherence will help to isolate these consistent linear relations. Many optimum filters for estimating the signal take account of these linear relations implicitly by weighting with the inverse of the spectral noise matrix. However, one cannot tell whether the coherent noise involved is due to noise generating events which cannot be predicted or controlled. Thus, the filters must be recalculated over a period of noise recording immediately prior to the arrival of each single signal. Part of the coherent noise generated within the array may be due to various causal factors for a particular array. If so, we can learn something about these factors by examining the linear relations between the various array elements. A potential benefit here is that a consistent linear model relating the different sub-elements would eliminate the need for computing a different set of filter coefficients for each event.

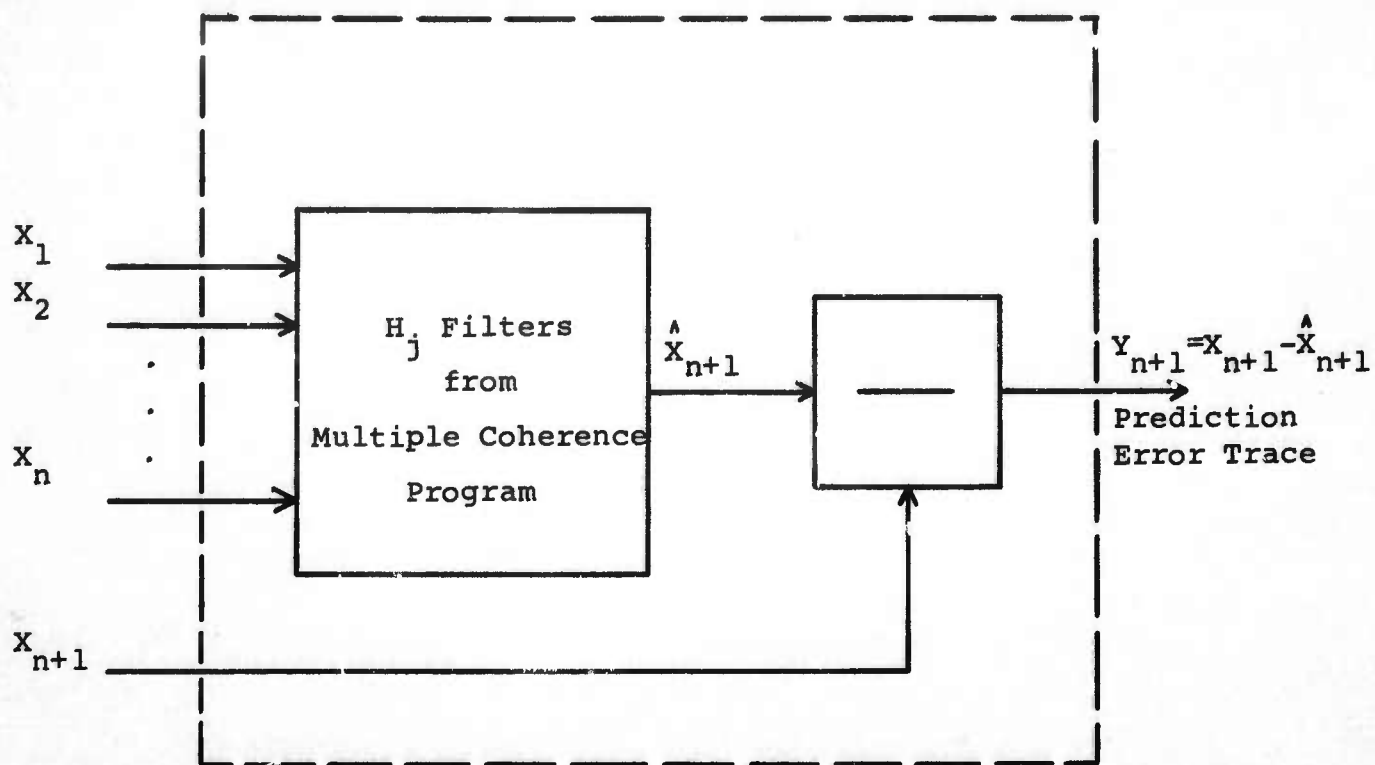
The multiple coherence function can indicate how many seismometer outputs in an array are necessary to properly determine the seismic noise field. If there are n independent seismic noise components, then the multiple coherence function would be unity when $(n + 1)$ st seismometers are placed in an array to measure seismic noise records. If part of the background is

composed of incoherent noise, then the multiple coherence function would indicate the percentage of coherent noise present and the number of seismometers necessary to define this coherent noise. The filter relations determined by the multiple coherence computations can then be used in array summation to bring the noise into destructive interference.*

This analysis does not guarantee that such optimum processing is possible. For example, if the noise and signal propagation characteristics across the array are identical, no velocity filtering scheme can be expected to separate the two even though the multiple coherence might be unity.

The multiple coherence function is the frequency domain equivalent of the prediction error filter in time. If n input seismic traces predict the $(n + 1)$ st trace in an array completely, then the multiple coherence will be unity and a prediction error filter could be used to exactly predict this $(n + 1)$ st output. In fact, linear filter relations derived by the multiple coherence program produce an estimate of the $(n + 1)$ st trace which, when subtracted from the actual $(n + 1)$ st trace, given a prediction error trace. Thus the combination of the filter derived in the multiple coherence program and the subtraction operation produces a prediction error filter as shown in the following diagram.

*For the mathematical description of the multiple coherence computation see Appendix I.



Prediction Error Filter

The objective of this study is to use the multiple coherence function to estimate the degree of predictability of the short period noise field at three deep well sites; UBSO, GV-TX and AP--OK.

2. DESCRIPTION OF DATA

We computed the multiple coherence of short period vertical component data from three vertical arrays. The first is at UBSO and includes a near-surface instrument in a 250 foot hole located 4000 feet from the well, plus six downhole instruments from 4000 to 9000 feet. The second is from GV-TX and includes a surface instrument at the well plus six downhole instruments from 4500 to 9500 feet. The third is from AP-OK and includes a surface instrument at the well plus one at 50 feet and four downhole instruments from 5500 to 9500 feet.

The sampling rate for the data is 10 samples per second. The number of points in the samples vary but are all between 3 to 3.5 minutes. The frequency range is from 0.1 to 2.6 cps with a frequency increment of 0.1 cps.

We varied the number of input channels in our multiple coherence computations from 2 to 6. We grouped the seismometers in two ways. For one group we used the surface instrument as the output and the other instruments as inputs. For the second group we used the bottom instrument as output channel and the other six as inputs. In each case the inputs furthest from the output channel were added first.

We examined two noise samples each from UBSO and AP-OK and one noise sample from GV-TX. At AP-OK one sample was long enough to make three successive samples of 3.5 minutes. All stationarity computations were made on these samples.

3. RESULTS

Multiple Coherence

On all of the multiple coherence plots in this report the output trace is either from the surface seismometer or the deepest seismometer. The ordering of the input channels starts with the furthest seismometers away from the output. On each of the multiple coherence plots a diagram of the instrument locations in the vertical array for that site is shown on the lower right. The inputs are listed in order of their addition to the multiple coherence computations.

Figure 1 shows multiple coherence versus frequency for the two output cases from data recorded at UBSO on 3 December 1966. The upper diagram shows multiple coherence with a surface instrument as output. The multiple coherence over most of the frequency range is generally low. Even at the microseismic frequencies (0.2 to 0.5 cps) the multiple coherence is less than .6 with all six downhole instruments used as inputs. This result shows that none of the downhole instruments correlate very well with the surface instrument. An exception occurs at 1.9 cps where the multiple coherence is high even for two inputs.

The lower diagram shows the multiple coherence with the deepest instrument as output. The multiple coherence is high throughout most of the frequency range, and especially so for 4 and 5 inputs when the deepest instrument is the output channel. The strong coherence at 1.9 cps shows up again but is not so evident since coherence at other frequencies is also

high. The multiple coherence increases with increasing number of inputs. The last inputs added are the ones closest to the output (deepest) seismometers. Over the range 1.0 to 1.8 cps correlation is high between seismometers separated by 2000 and 4000 feet but decreases considerably for seismometers separated by 6000 feet or more.

Figure 2 shows multiple coherence versus frequency for the two output cases on 7 January 1967. As in Figure 1, the upper diagram uses the surface instrument as the output and the lower diagram uses the deepest instrument as the output. The results in Figures 1 and 2 agree everywhere except that the highly correlated noise at 1.9 cps is not present on the 7 January 1967 sample.

Figure 3 shows multiple coherence versus frequency for data recorded at GV-TX on 20 March 1965. Again the upper diagram uses the surface seismometer as output and the lower diagram uses the deepest seismometer as output. The downhole traces at GV-TX correlate well with the surface trace for the microseisms (0.2 to 0.5 cps) especially with 3 or more inputs. However, the correlation of the downhole traces with the surface trace over the remainder of the frequency range is low.

With the deepest trace as output the multiple coherence with all 5 inputs is high (about 0.9) throughout the entire frequency range (0.1 to 2.6 cps). The multiple coherence increases significantly as inputs closer to the output are added. Furthermore, the multiple coherence at GV-TX with closest input 2000 feet from the output seismometer (the 4 input case) agrees

closely with the final multiple coherence for UBSO where the closest input is 2000 feet from the output seismometer. Thus coherence over the signal band in these vertical arrays decreases with increasing seismometer separation with very strong coherence for separation of only 1000 feet.

Figure 4 shows multiple coherence at AP-OK using surface trace as output for two time samples $3\frac{1}{2}$ minutes long with a 3 minute gap between them. The multiple coherence for the microseismic band (0.2 to 0.5 cps) is high for any number of inputs. The multiple coherence over the signal band (1.0 to 1.5) cps is low for 4 inputs or less. There is a significant increase in multiple coherence at 1.7 cps. When the last input trace, only 50 feet from the output surface seismometer, is added, the multiple coherence becomes high (greater than 0.9) for all frequencies. These two traces are recording essentially the same data.

Figure 5 shows multiple coherence using the deepest trace as output for the same neighboring time samples shown in Figure 4. The results on Figure 5 agree with those on Figure 4 with two exceptions. The first is that the final multiple coherence does not stay above 0.9 everywhere since no input is closer than 2000 feet to the output. The second is that larger multiple coherence occurs over the signal band (1.0 to 1.5 cps) than in Figure 4 showing that the downhole traces correlate with each other more than with the surface trace.

Figure 6 shows similar multiple coherence using a surface trace and a deepwell trace as outputs for AP-OK data recorded on 12 May 1965. In both examples the multiple coherence is low until the closest seismometer to the output seismometer is added to the inputs.

Figures 7, 8, and 9 show the ranges for input and output power spectra for the UBSO, GV-TX and AP-OK vertical arrays respectively. The spectra from all of these wells show a significant noise peak near 2 cps.

Stationarity Tests

Figures 10 and 11 show the expected db reduction in noise when prediction error filters are applied to three successive samples of 3 minutes each recorded at AP-OK. Figure 10 uses the deepest instrument as output. Figure 11 uses the surface instrument as output. Over the microseismic band (0.2 to 0.5 cps) the expected noise reduction inside the fitting interval varies between 16 and 22 db and outside the fitting interval within 2 db of this value. Over the signal band the expected noise reduction is less varying between 8 and 14 db when the deep instrument is output and between 2 and 7 db when the surface instrument is output within the fitting interval. The expected noise reduction is nearly as good outside the fitting interval. The strong correlations near 2 cps show expected noise reductions and stationarity properties similar to the noise in the signal band.

These tests show that the noise correlation in vertical arrays is much higher than correlations over surface arrays. Over three successive noise samples, at least, the noise seems to be strong. The stationarity test again shows that the deep instrument correlates with the others better than the surface instrument since the expected noise reduction is greater with the deep instrument as output.

4. CONCLUSIONS

1. The multiple coherence properties of the noise at the three vertical arrays with similar geometries are similar. At all three sites the downhole channels correlate with each other better than with the surface channel. At all three sites the coherence between downhole seismometers decreases markedly as their separation increases.

2. When the deep trace is the output and all seismometers are added as inputs, the multiple coherence is highest at GV-TX. In fact it is greater than .85 for all frequencies from .1 to 2.5 cps. For the AP-OK and UBSO wells the multiple coherence varies between .6 to .9 for most frequencies greater than .5 cps.

3. All three sites show a significant 2 cps component in the noise spectra for most of the examples tested. The multiple coherence of this 2 cps component is high but not appreciably higher than other noise frequencies above the microseismic band. Even the surface trace correlates well with the downhole traces for the 2 cps component.

4. The noise at AP-OK appears to be more stationary than noise at surface arrays. For three successive $3\frac{1}{2}$ minute samples the expected noise reduction from a prediction error filter applied in the fitting interval was 16 to 20 db over the microseismic band and between 2 and 7 db for frequencies greater than 0.5 cps. Outside the fitting interval the expected noise reduction was within 2 db of these values.

FIGURES

1. Multiple coherence versus frequency for a UBSO sample recorded in December 1966. The upper diagram uses the surface instrument as output; the lower uses the deepest instrument as output.
2. Multiple coherence versus frequency for a UBSO sample recorded in January 1967. The upper diagram uses the surface instrument as output; the lower uses the deepest instrument as output.
3. Multiple coherence versus frequency for a GV-TX sample recorded in March 1965. The upper diagram uses the surface instrument as output; the lower uses the deepest instrument as output.
4. Multiple coherence versus frequency at AP-OK for two samples 3 minutes apart. The surface instrument is the output.
5. Multiple coherence versus frequency at AP-OK for the same samples shown in Figure 4 but with the deepest instrument as the output.
6. Multiple coherence versus frequency at AP-OK for a sample recorded in May 1965. The upper diagram uses the surface instrument as output; the lower uses a deep instrument as output.
7. The output and range of input power spectra for samples recorded at UBSO in December 1966.
8. The output and range of input power spectra for samples recorded at GV-TX in December 1966.
9. The output and range of input power spectra for samples recorded at AP-OK in December 1966.
10. Expected db reduction in noise when prediction error filters are applied to three successive samples at AP-OK. The fitting interval is the Time 1 sample. The deepest instrument is output.
11. Expected db reduction in noise when prediction error filters are applied to three successive samples at AP-OK. The fitting interval is the Time 1 sample. The surface instrument is output.

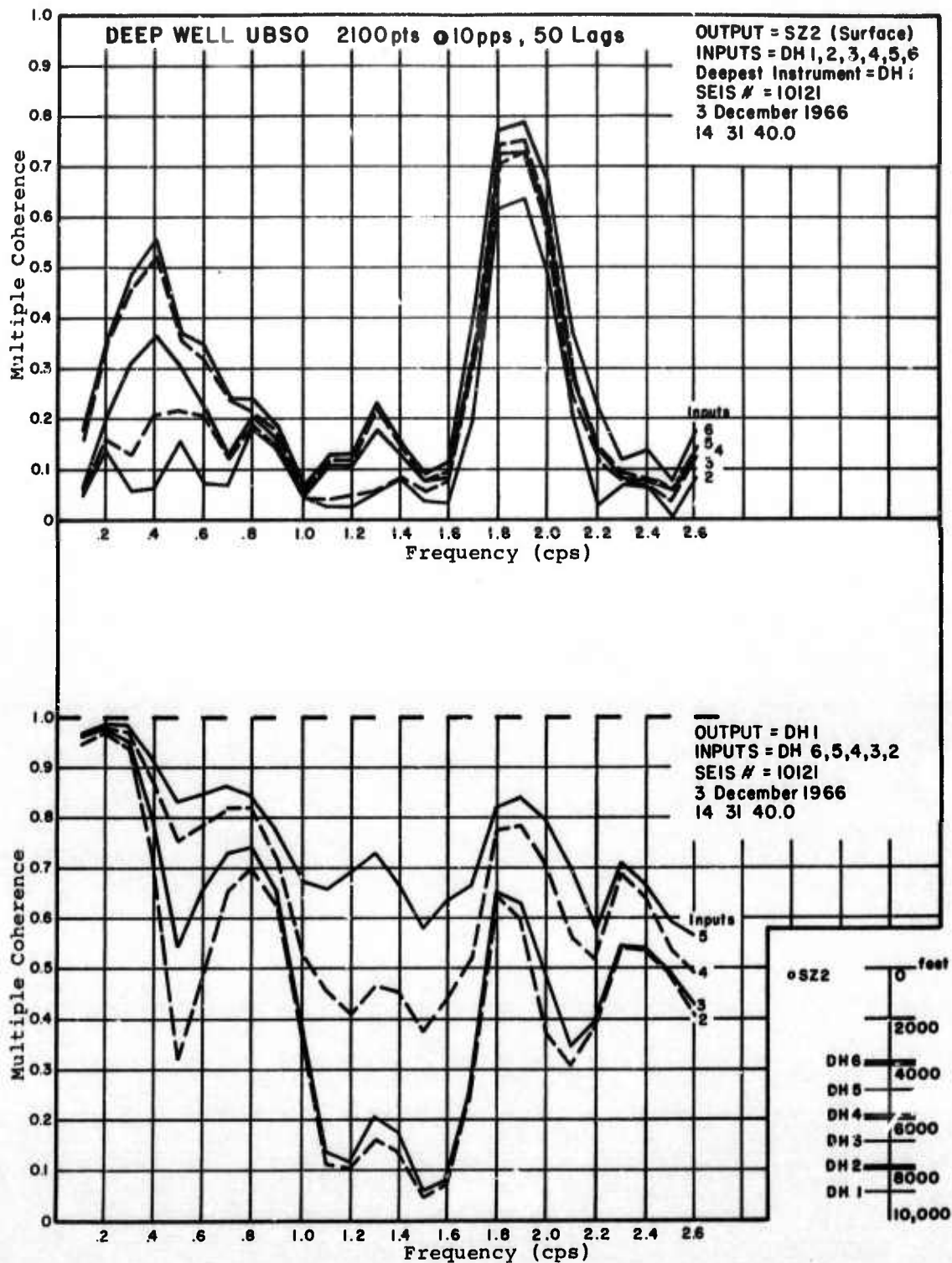


Figure 1. Multiple coherence versus frequency for a UBSO sample recorded in December 1966. The upper diagram uses the surface instrument as output; the lower uses the deepest instrument as output.

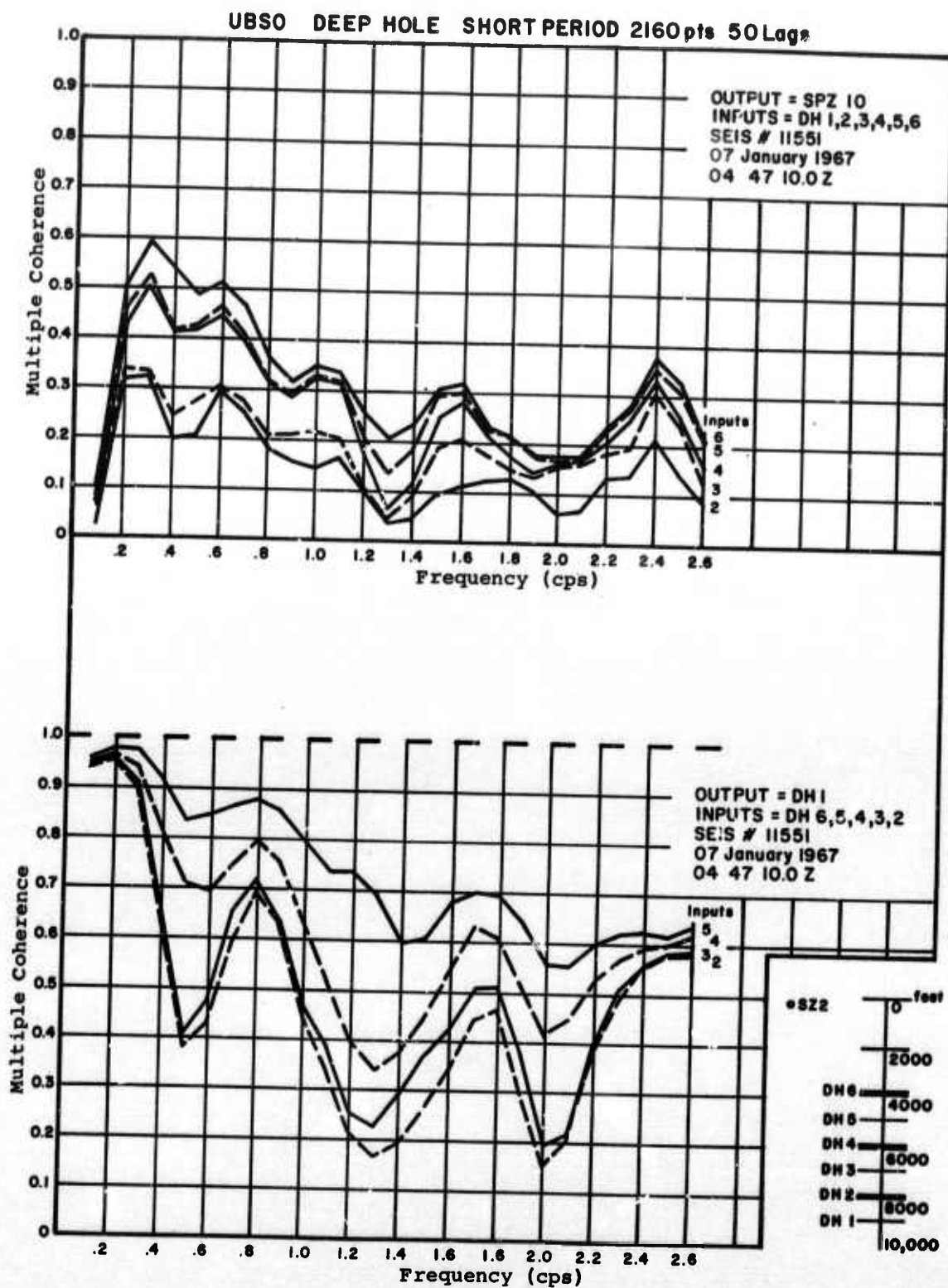


Figure 2. Multiple coherence versus frequency for a UBSO sample recorded in January 1967. The upper diagram uses the surface instrument as output; the lower uses the deepest instrument as output.

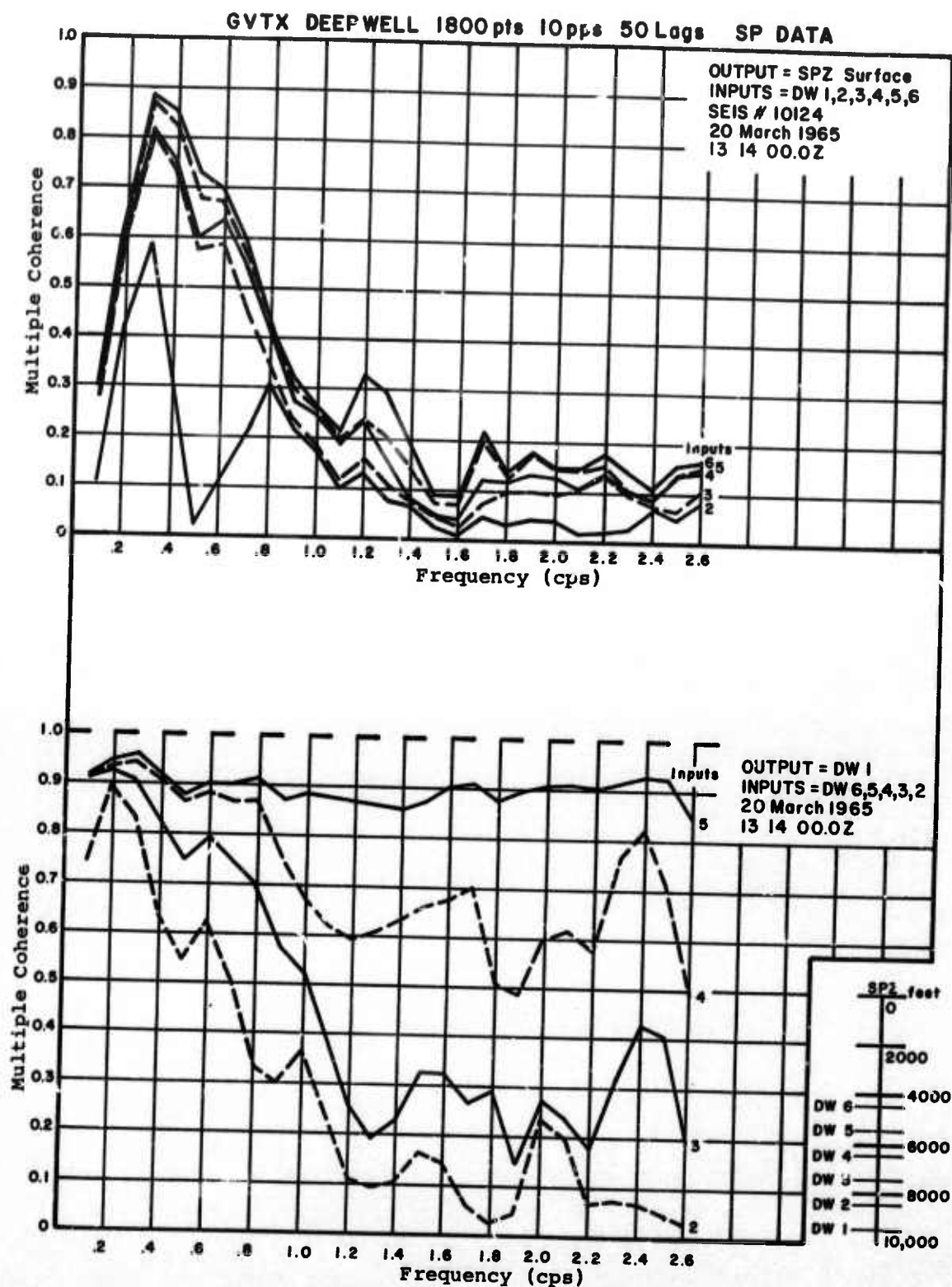


Figure 3. Multiple coherence versus frequency for a GV-TX sample recorded in March 1965. The upper diagram uses the surface instrument as output; the lower uses the deepest instrument as output.

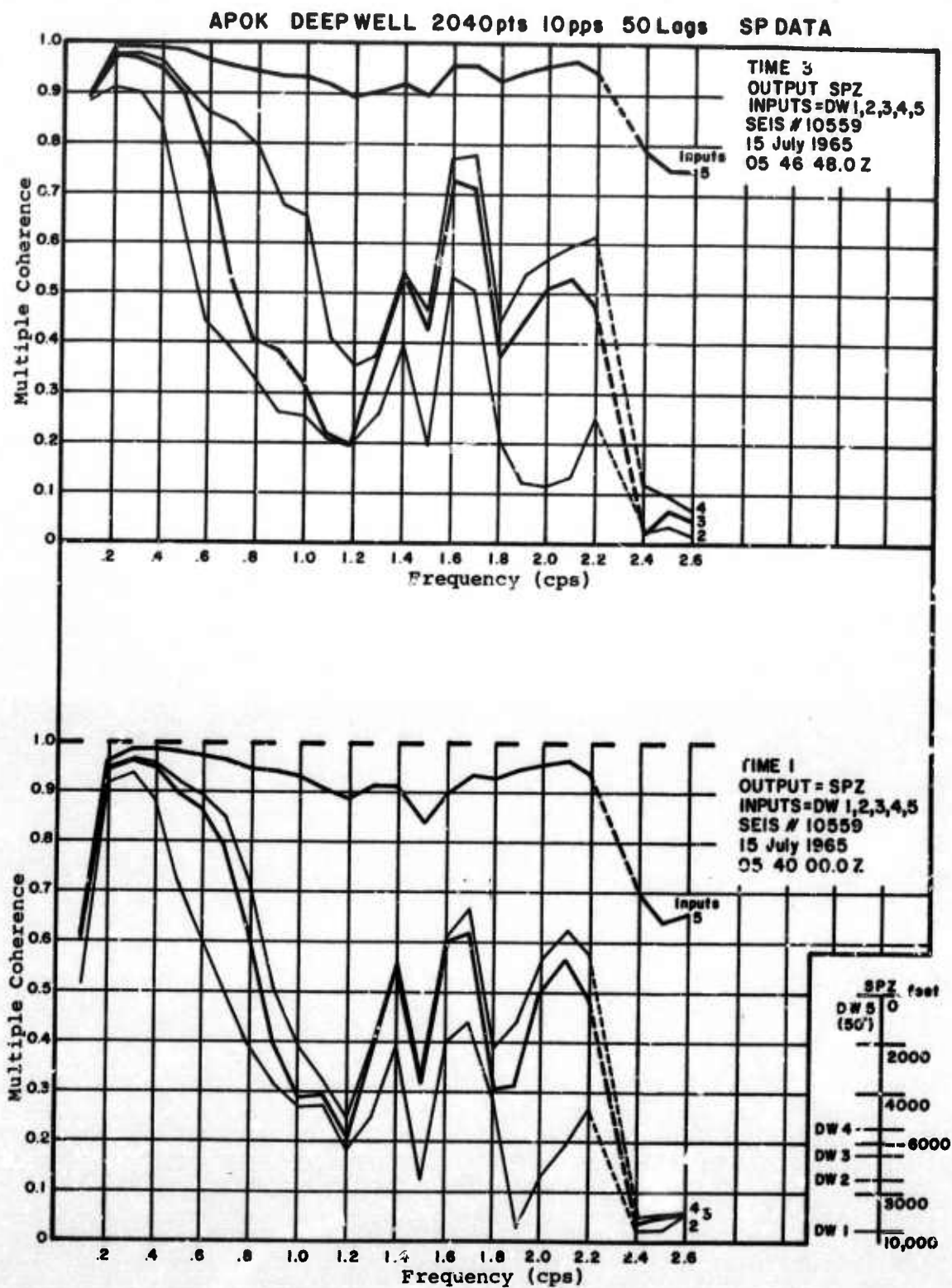


Figure 4. Multiple coherence versus frequency at AP-OK for two samples 3 minutes apart. The surface instrument is the output.

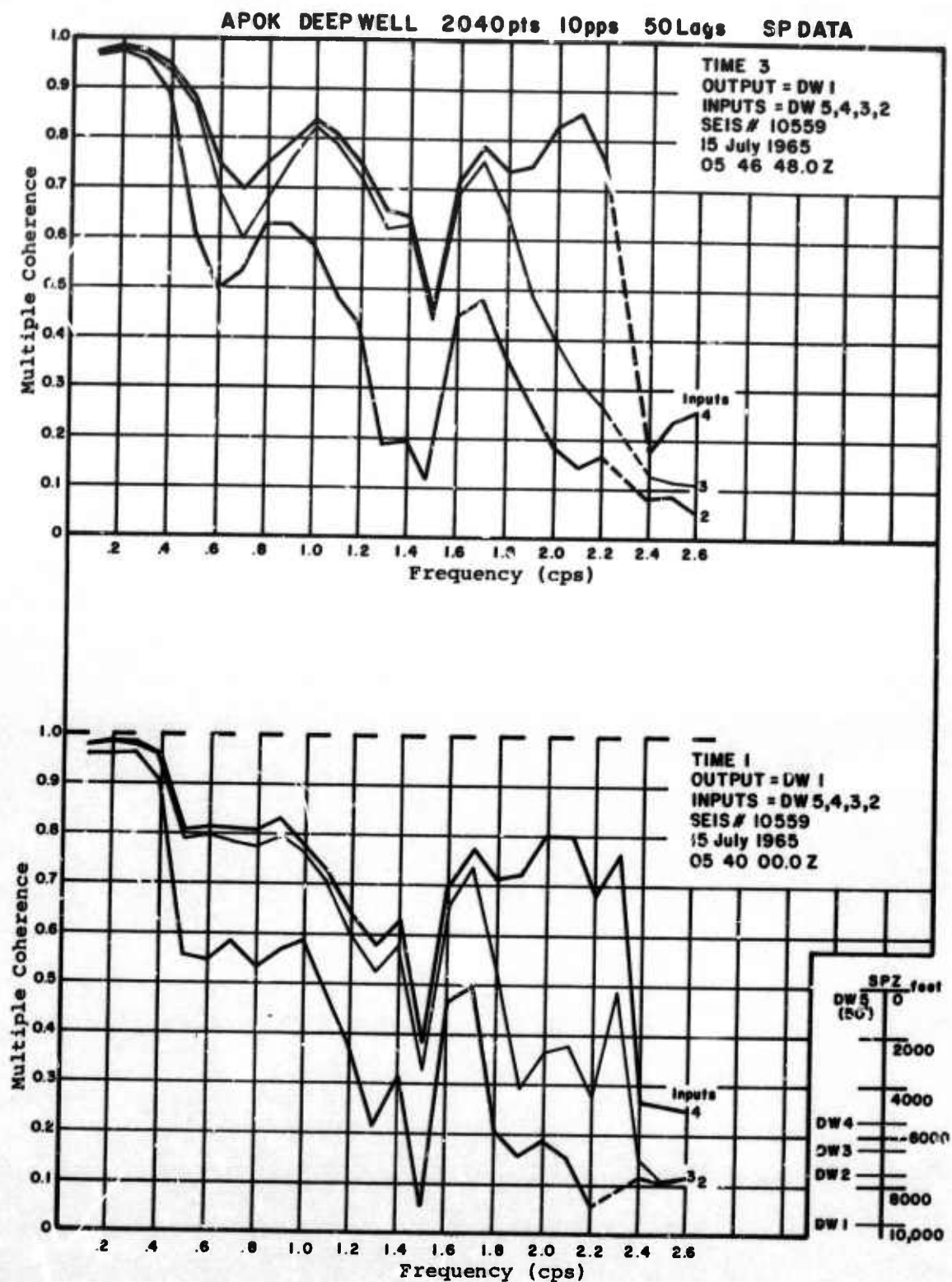


Figure 5. Multiple coherence versus frequency at APOK for the same samples shown in Figure 4 but with the deepest instrument as the output.

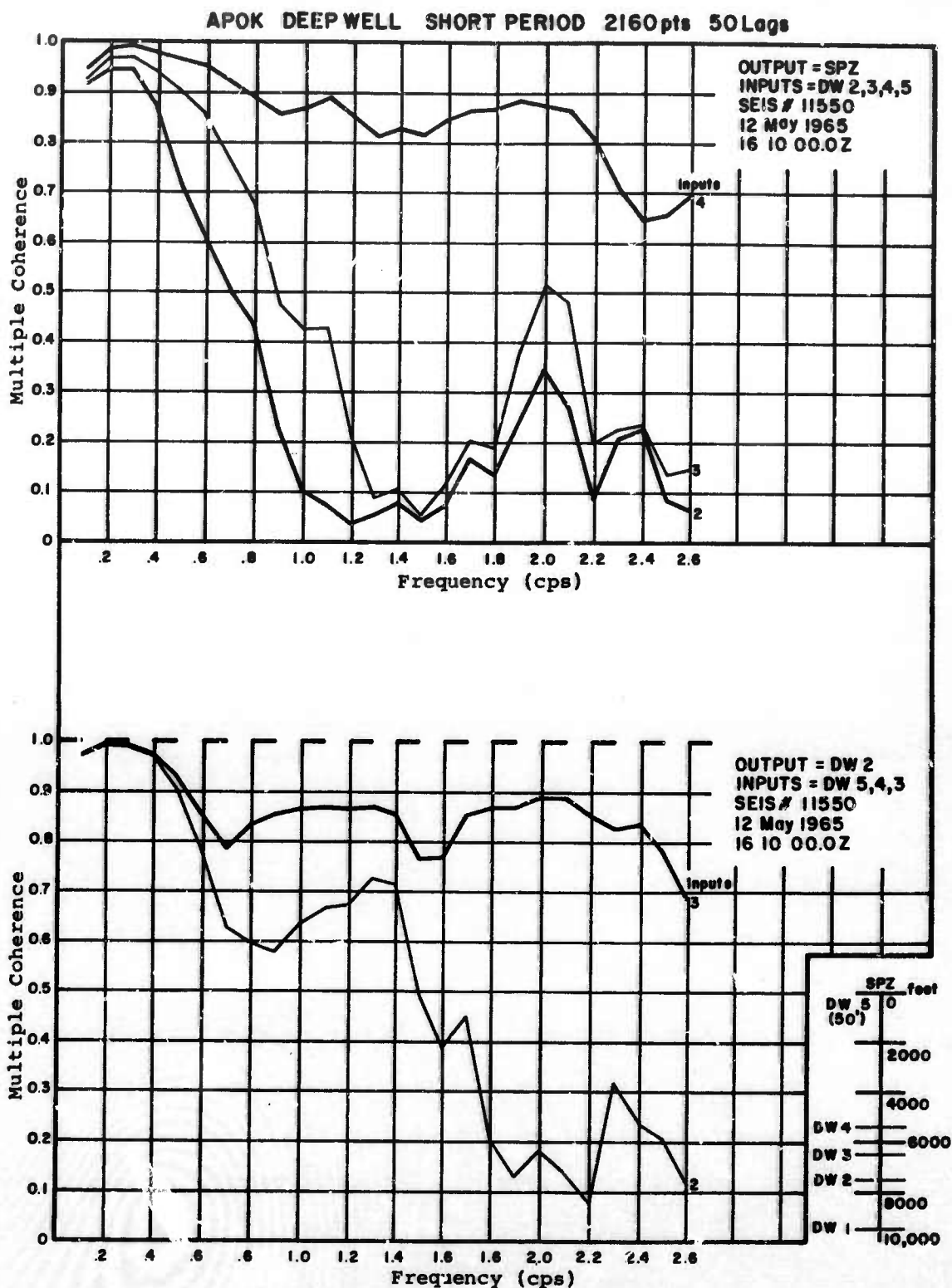


Figure 6. Multiple coherence versus frequency at AP-OK for a sample recorded in May 1965. The upper diagram uses the surface instrument as output; the lower uses a deep instrument as output.

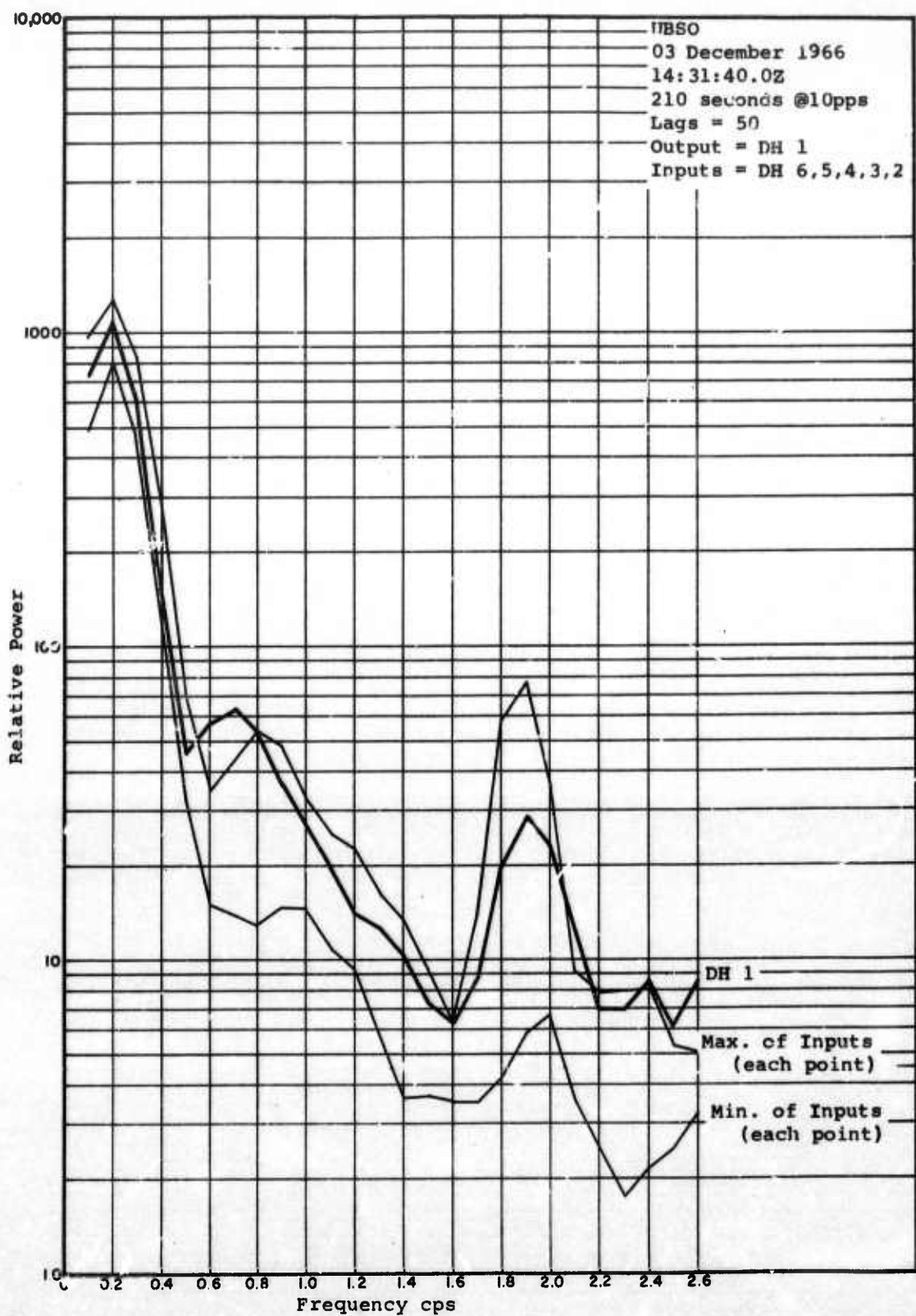


Figure 7. The output and range of input power spectra for samples recorded at UBSO In December 1966.

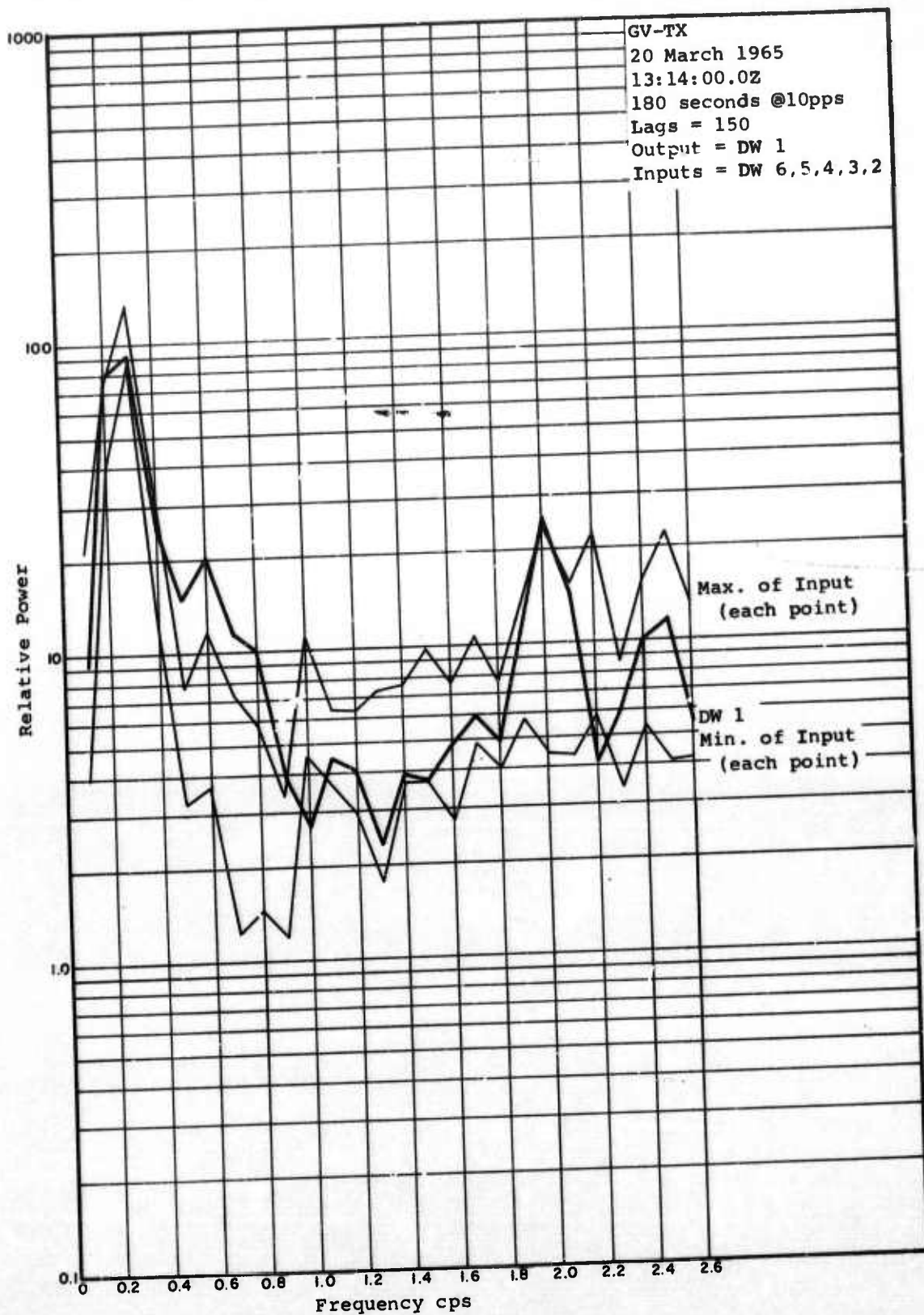


Figure 8. The output and range of input power spectra for samples recorded at GV-TX in December 1966.

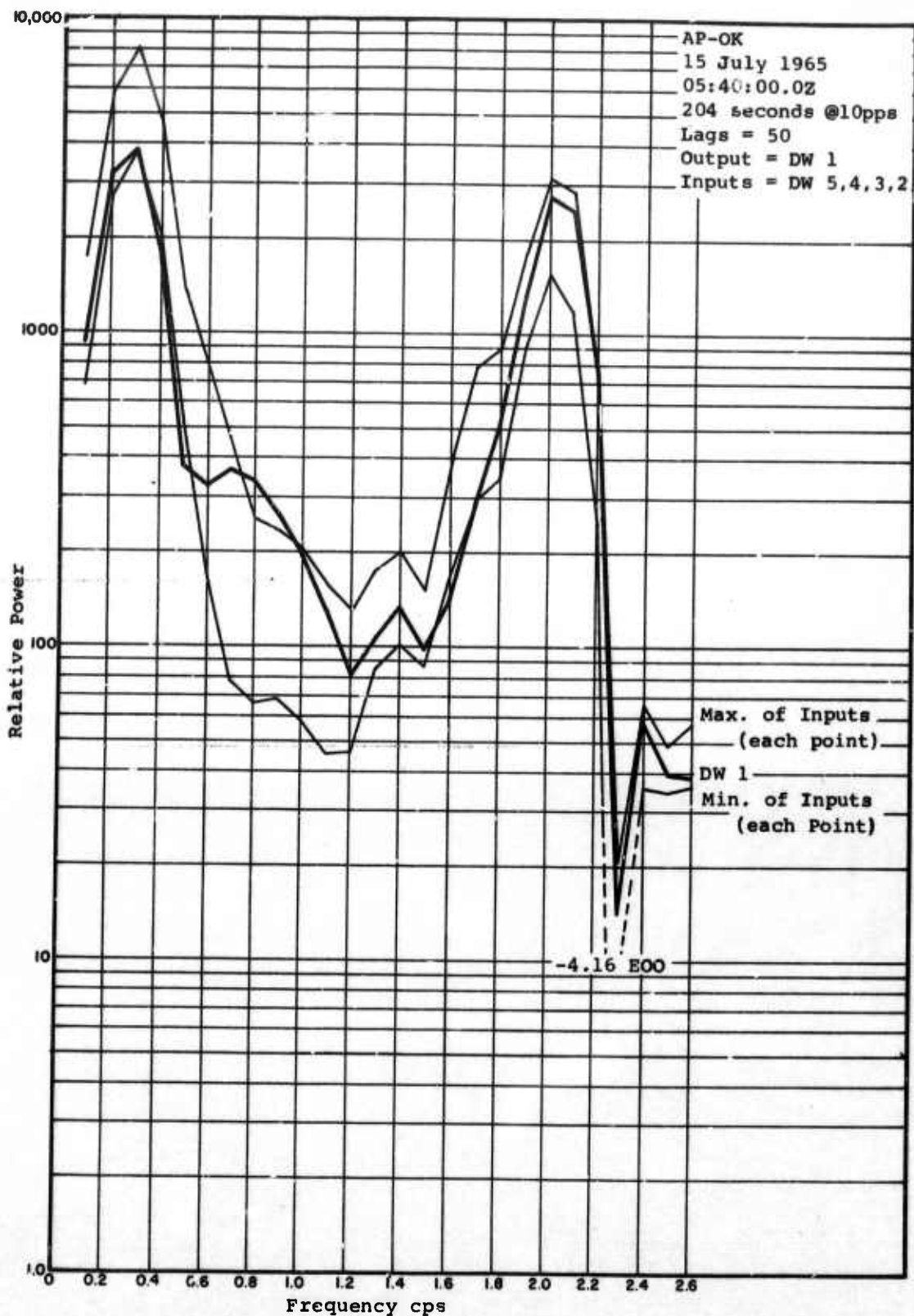


Figure 9. The output and range of input power spectra for samples recorded at AP-OK in December 1966.

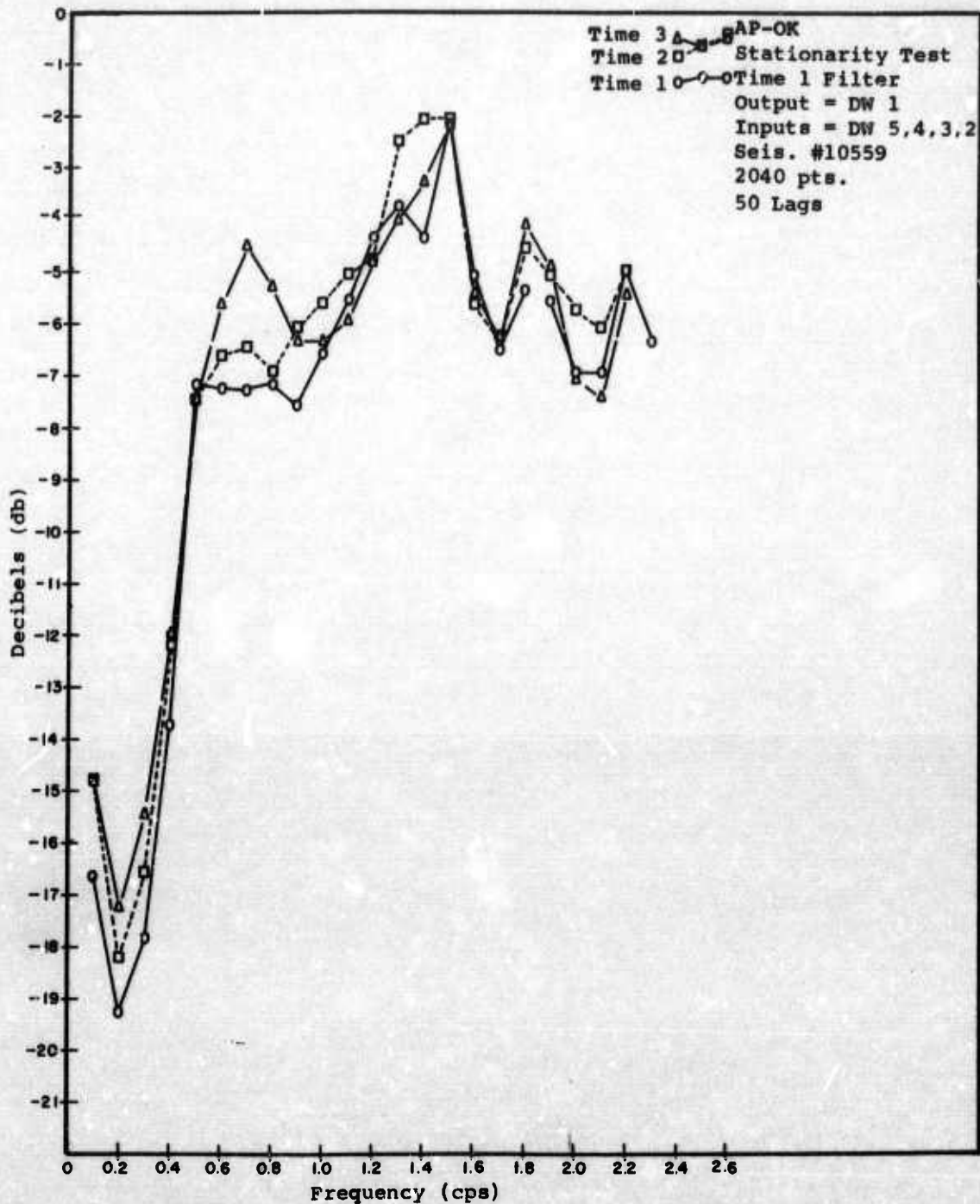


Figure 10. Expected db reduction in noise when prediction error filters are applied to three successive samples at AP-OK. The fitting interval is the Time 1 sample. The deepest instrument is output.

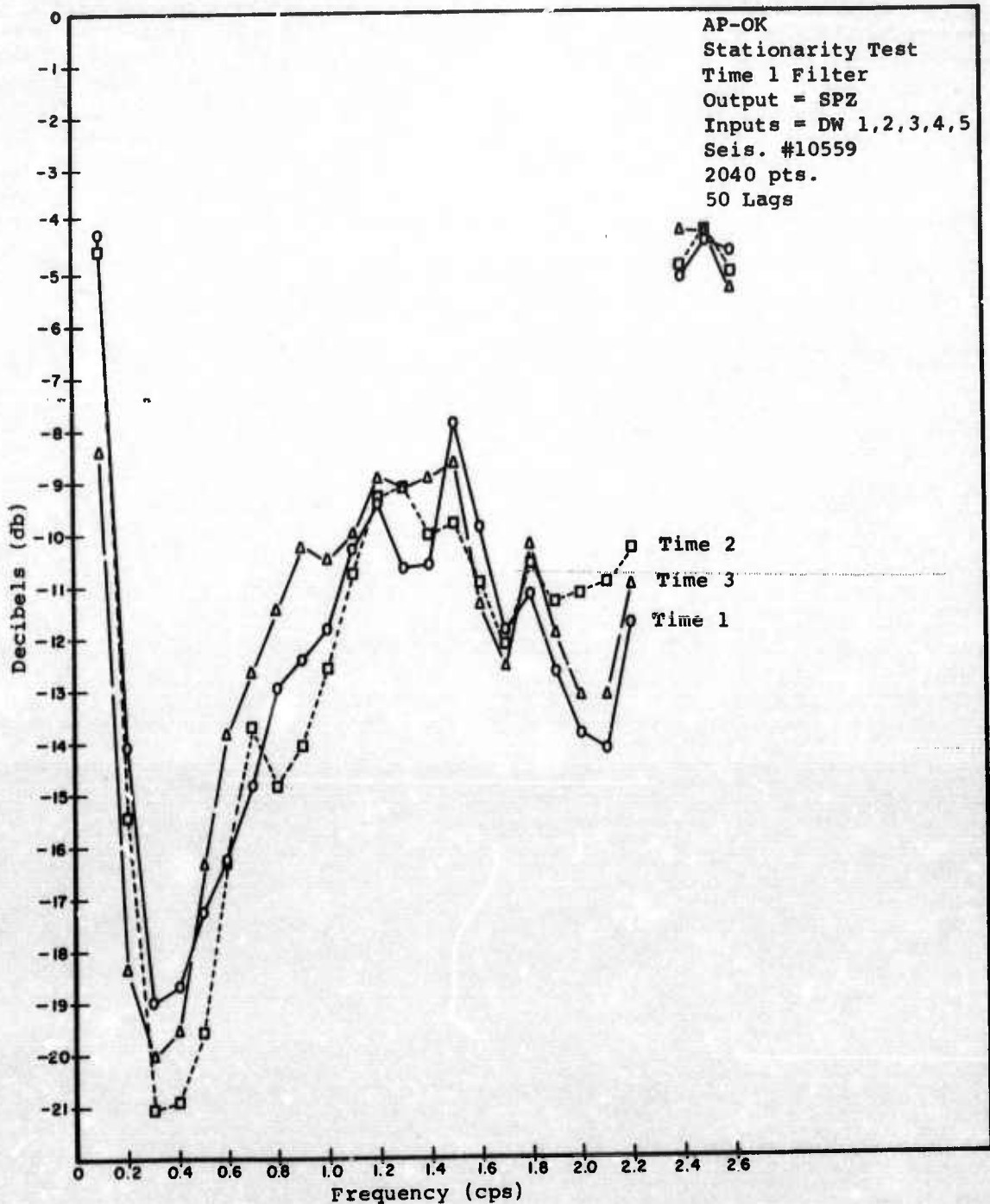


Figure 11. Expected db reduction in noise when prediction error filters are applied to three successive samples at AP-OK. The fitting interval is the Time 1 sample. The surface instrument is output.

APPENDIX I

*Multiple Coherence Functions

Consider a collection of q clearly defined inputs $x_i(t)$; $i = 1, 2, \dots, q$, and one output $y(t)$, as pictured in Figure 5.12. Let $G_i(f) = G_{ii}(f)$ be the

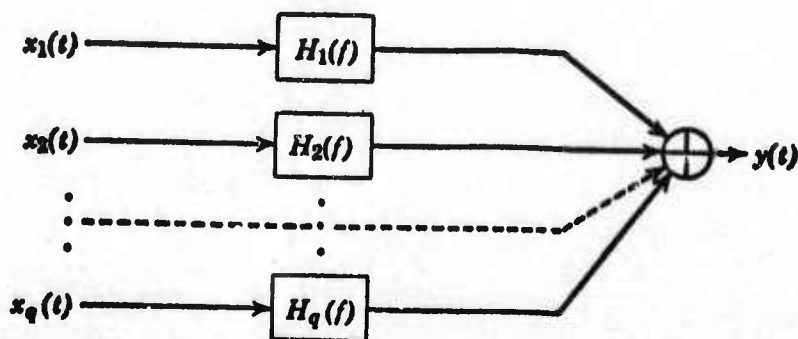


Figure 5.12 Multiple-input linear system.

power spectral density function for $x_i(t)$, and $G_{ij}(f)$ be the cross-spectral density function between $x_i(t)$ and $x_j(t)$. Define the $N \times N$ spectral matrix by

$$G_{xx}(f) = \begin{bmatrix} G_{11}(f) & G_{12}(f) & \cdots & G_{1q}(f) \\ G_{21}(f) & G_{22}(f) & & G_{2q}(f) \\ \vdots & \vdots & & \vdots \\ G_{q1}(f) & G_{q2}(f) & & G_{qq}(f) \end{bmatrix} \quad (1)$$

*This explanation of multiple coherence functions was taken from "Measurement and Analysis of Random Data", Bendat, J. S., and Piersol, A. G., John Wiley and Sons, 1966. For more detailed theoretical developments and discussions of multiple, partial and marginal coherence functions, see this text.

The ordinary coherence function between $x_i(f)$ and $x_j(f)$ is defined by

$$\gamma_{ij}^2(f) = \frac{|G_{ij}(f)|^2}{G_i(f) G_j(f)} \quad (2)$$

The multiple coherence function between $x_i(f)$ and all other inputs $x_1(f), x_2(f), \dots$, excluding $x_i(f)$, is defined by

$$\gamma_{i..}^2(f) = 1 - [G_i(f) G'(f)]^{-1} \quad (3)$$

where $G^i(g)$ denotes the i th diagonal element of the inverse matrix $G_{xx}^{-1}(f)$ associated with Eq. (1). The ordinary and multiple coherence functions are both real-valued quantities which are bounded by zero and unity. That is,

$$\begin{aligned} 0 &\leq \gamma_{ij}^2(f) \leq 1 \\ 0 &\leq \gamma_{i..}^2(f) \leq 1 \end{aligned} \quad (4)$$

The multiple coherence function is a measure of the linear relationship between the time history at one point, and the time histories at the collection of other points. That is, the multiple coherence function indicates whether or not the data at all of the other points linearly produce the results at a given point.

APPENDIX 2

Theoretical Development of The Stationarity Relations

A. Noise Reduction Within The Fitting Interval

A number of useful statistical measures such as ordinary and multiple coherence can be used as tools to indicate the amount of noise reduction feasible in a multiply coherent array. The basic linear model which determines the db reduction possible in the noise field by multiple coherence filtering relates a reference element (trace) $y(t)$ of an array to the other elements, say $x_1(t)$, $x_2(t)$, ..., $x_p(t)$ in the array through the linear model

$$y(t) = \sum_{k=1}^P \int_{-\infty}^{\infty} h_k(\alpha) x_k(t-\alpha) d\alpha \quad (1)$$

Generally we determine $h_k(t)$ as the time invariant linear filter that makes the mean square error between $y(t)$ and its predicted value a minimum, i. e.

$$E \left| y(t) - \sum_{k=1}^P \int_{-\infty}^{\infty} h_k(\alpha) x_k(t-\alpha) d\alpha \right|^2 = \min \quad (2)$$

which, by the usual orthogonality principle (see Papoulis 1), yields the condition

$$E y(t) x_l(t+\tau) = \sum_{k=1}^P \int_{-\infty}^{\infty} h_k(\alpha) E x_k(t-\alpha) x_l(t+\tau) d\alpha$$

$$l = 1, 2, \dots, p, -\infty < \tau < \infty \quad (3)$$

$$\text{or} \quad R_{yx\ell}(\tau) = \sum_{k=1}^P \int h_k(\alpha) R_{x_k x_\ell}(\tau + \alpha) d\alpha \quad (4)$$

which by taking Fourier transforms implies that

$$S_{yx\ell}(\omega) = \sum_{k=1}^P H_k^*(\omega) S_{x_k x_\ell}(\omega) \quad (5)$$

Now, the mean square error can be written

$$\begin{aligned} E|y(t) - \sum_{k=1}^P \int h_k(\alpha) x_k(t-\alpha) d\alpha|^2 &= E \left(y(t) - \sum_{k=1}^P \int_{-\infty}^{\infty} h_k(\alpha) x_k(t-\alpha) d\alpha \right) y(t) \\ &= R_{yy}(0) - \sum_{k=1}^P \int h_k(\alpha) R_{x_k y}(\alpha) d\alpha \\ &= \int_{-\infty}^{\infty} \left[S_{yy}(\omega) - \sum_{k=1}^P H_k^*(\omega) S_{x_k y}(\omega) \right] \frac{d\omega}{2\pi} \\ &= \int_{-\infty}^{\infty} \left(S_{yy} - \frac{S_{yx}}{S_{xx}} S_{xx}^{-1} S_{xy} \right) (\omega) \frac{d\omega}{2\pi} \\ &= \int_{-\infty}^{\infty} (1 - \alpha^2(\omega)) S_{yy}(\omega) \frac{d\omega}{2\pi} \quad (6) \end{aligned}$$

where $\alpha^2(\omega)$ is the multiple coherence and $(1 - \alpha^2(\omega))$ measures the reduction in power possible at the frequency ω . With $\alpha^2(\omega) = 1$ the mean square error is zero and with $\alpha^2(\omega) = 0$ the mean square error is just

$$\int_{-\infty}^{\infty} S_{yy}(\omega) \frac{d\omega}{2\pi} = R_{yy}(0) = E|y(t)|^2 \quad (7)$$

which is the original power in the process $y(t)$. Now the quantity $(1 - \alpha^2(\omega)) S_{yy}(\omega)$ represents the residual power at each frequency after the best linear estimate of the form (1) has been subtracted out. Hence the db reduction in power at each frequency is just the ratio of the output power of the residual (see equation (2)) to the input power in $y(t)$ or

$$I_H(\omega) = 10 \log \frac{S_{ee}(\omega)}{S_{yy}(\omega)} = 10 \log (1 - \alpha^2(\omega)) \quad (8)$$

where $\alpha^2(\omega)$ is the multiple coherence and $S_{ee}(\omega)$ is the power spectrum of the error process

$$e(t) = y(t) - \sum_{k=1}^P \int_{-\infty}^{\infty} h_k(\alpha) x_k(t - \alpha) d\alpha \quad (9)$$

B. Noise Reduction Outside The Fitting Interval

We would also like to determine the noise reduction in db which would result from using a set of filters $g_k(t)$, $k=1, \dots, P$ which have been derived either from another fitting interval or from theoretical considerations. To accomplish this let $h_k(t)$ be the optimal filters for the time under investigation and let $g_k(t)$ be any other set of filters whose mean square error is to be compared with $h_k(t)$. The mean square error of the g filters can be written using the orthogonality principle as

$$E \left| y(t) - \sum_{k=1}^P \int_{-\infty}^{\infty} g_k(\alpha) x_k(t - \alpha) d\alpha \right|^2 =$$

$$\begin{aligned}
& E \left| y(t) - \sum_{k=1}^P \int_{-\infty}^{\infty} h_k(\alpha) x_k(t-\alpha) d\alpha + \sum_{k=1}^P \int_{-\infty}^{\infty} (h_k(\alpha) - g_k(\alpha)) x_k(t-\alpha) d\alpha \right|^2 \\
&= E \left| y(t) - \sum_{k=1}^P \int_{-\infty}^{\infty} h_k(\alpha) x_k(t-\alpha) d\alpha \right|^2 + E \left| \sum_{k=1}^P \int_{-\infty}^{\infty} (h_k(\alpha) - g_k(\alpha)) x_k(t-\alpha) d\alpha \right|^2 \\
&= \int_{-\infty}^{\infty} (1 - \alpha^2(\omega)) S_{YY}(\omega) \frac{d\omega}{2\pi} + \int_{-\infty}^{\infty} (\underline{H} - \underline{G})^* S_{XX} (\underline{H} - \underline{G}) (\omega) \frac{d\omega}{2\pi} \\
&= \int_{-\infty}^{\infty} \left[(1 - \alpha^2(\omega)) + \frac{(\underline{H} - \underline{G})^* S_{XX} (\underline{H} - \underline{G}) (\omega)}{S_{YY}(\omega)} \right] S_{YY}(\omega) \frac{d\omega}{2\pi} \quad (10)
\end{aligned}$$

Hence, if we call the new error $\ell'(t)$ we have

$$\ell'(t) = y(t) - \sum_{k=1}^P \int g_k(\alpha) x_k(t-\alpha) d\alpha$$

with power spectrum $S_{\ell', \ell'}(\omega)$, the new value for the improvement in the $S_k(t)$ filters would be

$$I_G(\omega) = 10 \log \frac{S_{\ell', \ell'}(\omega)}{S_{YY}(\omega)} = 10 \log_S \left(1 - \alpha^2(\omega) + \frac{(\underline{H} - \underline{G})^* S_{XX} (\underline{H} - \underline{G}) (\omega)}{S_{YY}(\omega)} \right) \quad (12)$$

Equation (12) shows that the improvement in the $g_k(t)$ filters is expressed in terms of the improvement in the $h_k(t)$ filters and a correction term which is zero when $\underline{H} = \underline{G}$.

The improvement values $I_H(w)$ and $I_G(w)$ in equations (8) and (12) are those shown in the main body of the report.

Reference

1. Papoulis, A., Probability, Random Variables, and Stochastic Processes, McGraw Hill, 1965.

Unclassified

Security Classification

DOCUMENT CONTROL DATA - R&D

(Security classification of title, body of abstract and indexing annotation must be entered when the overall report is classified)

1. ORIGINATING ACTIVITY (Corporate author)

TELEDYNE, INC.
ALEXANDRIA, VIRGINIA

2a. REPORT SECURITY CLASSIFICATION

Unclassified

2b. GROUP

3. REPORT TITLE

MULTIPLE COHERENCE OF NOISE AT 3 VERTICAL ARRAYS UBSO, GV-TX, AP-OK

4. DESCRIPTIVE NOTES (Type of report and inclusive dates)

Scientific

5. AUTHOR(S) (Last name, first name, initial)

Chiburis, E. F. and Dean, W. C.

6. REPORT DATE

28 June 1967

7a. TOTAL NO. OF PAGES

30

7b. NO. OF REFS

1

8a. CONTRACT OR GRANT NO.

F. 33657-67-C-131

a. PROJECT NO.

VELA T/6702

c. ARPA Order No. 624

d. ARPA Program Code No. 5810

8a. ORIGINATOR'S REPORT NUMBER(S)

191

8b. OTHER REPORT NO(S) (Any other numbers that may be assigned this report)

10. AVAILABILITY/LIMITATION NOTICES

This document is subject to special export controls and each transmittal to foreign governments or foreign national may be made only with prior approval of Chief, AFTAC.

11. SUPPLEMENTARY NOTES

12. SPONSORING MILITARY ACTIVITY

ADVANCED RESEARCH PROJECTS AGENCY
NUCLEAR TEST DETECTION OFFICE
WASHINGTON, D. C.

13. ABSTRACT

Multiple coherence gives a quantitative measure versus frequency of how well a linear combination of n input channels can match the $(n + 1)$ st channel in a seismic array. If the inputs can match the output exactly, then the multiple coherence is unity and only n channels are necessary to describe the noise field. This report shows multiple coherence versus frequency at three vertical arrays of short period, vertical component seismometers. One of the seismic traces, either the surface trace or the deepest trace, is used as the output and 2 to 6 of the others are used as inputs.

The multiple coherence properties of the noise are similar at the three vertical arrays with similar geometries. At all three sites the downhole channels correlate with each other better than with the surface channel. At all three sites the coherence between downhole seismometers decreases markedly as their separation increases.

When the deep trace is the output and all seismometers are added as inputs, the multiple coherence is highest at GV-TX. The multiple coherence at GV-TX is greater than .85 for all frequencies from .1 to 2.5 cps. For the AP-OK and UBSO wells the multiple coherence varies between .6 to .9 for most frequencies greater than .5 cps.

DD FORM 1473
1 JAN 64

Unclassified

Security Classification

14. KEY WORDS	LINK A		LINK B		LINK C	
	ROLE	WT	ROLE	WT	ROLE	WT
Vertical Array						
Multiple Coherence						
Prediction Error						
Multi-channel Filtering						
Noise Spectra						
Seismic Arrays						
Stationarity						

INSTRUCTIONS

1. **ORIGINATING ACTIVITY:** Enter the name and address of the contractor, subcontractor, grantee, Department of Defense activity or other organization (corporate author) issuing the report.

2a. **REPORT SECURITY CLASSIFICATION:** Enter the overall security classification of the report. Indicate whether "Restricted Data" is included. Marking is to be in accordance with appropriate security regulations.

2b. **GROUP:** Automatic downgrading is specified in DoD Directive 5200.10 and Armed Forces Industrial Manual. Enter the group number. Also, when applicable, show that optional markings have been used for Group 3 and Group 4 as authorized.

3. **REPORT TITLE:** Enter the complete report title in all capital letters. Titles in all cases should be unclassified. If a meaningful title cannot be selected without classification, show title classification in all capitals in parentheses immediately following the title.

4. **DESCRIPTIVE NOTES:** If appropriate, enter the type of report, e.g., interim, progress, summary, annual, or final. Give the inclusive dates when a specific reporting period is covered.

5. **AUTHOR(S):** Enter the name(s) of author(s) as shown on or in the report. Enter last name, first name, middle initial. If military, show rank and branch of service. The name of the principal author is an absolute minimum requirement.

6. **REPORT DATE:** Enter the date of the report as day, month, year; or month, year. If more than one date appears on the report, use date of publication.

7a. **TOTAL NUMBER OF PAGES:** The total page count should follow normal pagination procedures, i.e., enter the number of pages containing information.

7b. **NUMBER OF REFERENCES:** Enter the total number of references cited in the report.

8a. **CONTRACT OR GRANT NUMBER:** If appropriate, enter the applicable number of the contract or grant under which the report was written.

8b, 8c, & 8d. **PROJECT NUMBER:** Enter the appropriate military department identification, such as project number, subproject number, system numbers, task number, etc.

9a. **ORIGINATOR'S REPORT NUMBER(S):** Enter the official report number by which the document will be identified and controlled by the originating activity. This number must be unique to this report.

9b. **OTHER REPORT NUMBER(S):** If the report has been assigned any other report numbers (either by the originator or by the sponsor), also enter this number(s).

10. **AVAILABILITY/LIMITATION NOTICES:** Enter any limitations on further dissemination of the report, other than those

imposed by security classification, using standard statements such as:

- (1) "Qualified requesters may obtain copies of this report from DDC."
- (2) "Foreign announcement and dissemination of this report by DDC is not authorized."
- (3) "U. S. Government agencies may obtain copies of this report directly from DDC. Other qualified DDC users shall request through _____."
- (4) "U. S. military agencies may obtain copies of this report directly from DDC. Other qualified users shall request through _____."
- (5) "All distribution of this report is controlled. Qualified DDC users shall request through _____."

If the report has been furnished to the Office of Technical Services, Department of Commerce, for sale to the public, indicate this fact and enter the price, if known.

11. **SUPPLEMENTARY NOTES:** Use for additional explanatory notes.

12. **SPONSORING MILITARY ACTIVITY:** Enter the name of the departmental project office or laboratory sponsoring (paying for) the research and development. Include address.

13. **ABSTRACT:** Enter an abstract giving a brief and factual summary of the document indicative of the report, even though it may also appear elsewhere in the body of the technical report. If additional space is required, a continuation sheet shall be attached.

It is highly desirable that the abstract of classified reports be unclassified. Each paragraph of the abstract shall end with an indication of the military security classification of the information in the paragraph, represented as (TS), (S), (C), or (U).

There is no limitation on the length of the abstract. However, the suggested length is from 150 to 225 words.

14. **KEY WORDS:** Key words are technically meaningful terms or short phrases that characterize a report and may be used as index entries for cataloging the report. Key words must be selected so that no security classification is required. Identifiers, such as equipment model designation, trade name, military project code name, geographic location, may be used as key words but will be followed by an indication of technical context. The assignment of links, rules, and weights is optional.